J Mater Sci: Mater Med (2010) 21:1205–1210
DOI 10.1007/s10856-009-3881-3

Synthesis of PVP-coated ultra-small Fe_3O_4 nanoparticles as a MRI contrast agent

Ying Zhang · Jing-Ying Liu · Song Ma · Ya-Jing Zhang · Xiang Zhao · Xiang-Dong Zhang · Zhi-Dong Zhang

Received: 29 June 2009 / Accepted: 17 September 2009 / Published online: 7 February 2010

Abstract Ultra-small Fe_3O_4 nanoparticles were prepared by using the coprecipitation method, in which the polyvinylpyrrolidone (PVP) serves as a stabilizer. The nanoparticles were characterized by means of X-ray diffraction (XRD), transmission electron microscopy (TEM), infra spectrum (IR), X-ray photoelectron spectroscopy (XPS) and in vivo magnetic resonance imaging (MRI) test. The results showed that the particles' size was determined by the dripping rate and that PVP molecules played the role of preventing the aggregation and restricting the size of Fe_3O_4 nanoparticles. The Fe_3O_4 nanoparticles with diameter from 6.5 to 1.9 nm obviously exhibited negative contrast enhancement and concentrated at the target area guided by a permanent magnet.

1 Introduction

Magnetic nanoparticles (especially, iron-oxide nanoparticles) have attracted intensive attention in biomedical applications [1], such as separation of biomacromolecules [2], magnetic resonance imaging (MRI) [3], biological labels [4] and targeted drug delivery [5–7]. For these applications, magnetic particles should have a small size with a narrow size distribution. The smaller size the iron-oxide particles have, the more rapid reactivity and biodegradation the particles will present [8]. Therefore, the synthesis of ultra-small Fe_3O_4 nanoparticles with size less than 10 nm is highly desired for biomedical applications [9, 10]. Recently, several studies on the synthesis of ultra-small magnetic nanoparticles have been reported. Sun and Zeng [11] firstly reported simple organic-phase synthesis of magnetite nanoparticles with sizes variable from 3 to 20 nm in diameter. Liz et al. [12–16] employed water-in-oil microemulsion method to obtain magnetic iron-oxide nanoparticles with size less than 10 nm. However, a large amount of organic solvents was used in these synthesizing processes, which would lead to not only higher cost but also non-friendly to environment. The coprecipitation method, as an economic, biocompatible, and environmentally friend method, has been used for synthesizing Fe_3O_4 nanoparticles [17, 18], but ultra-small Fe_3O_4 nanoparticles have not been successfully synthesized by this method yet.

In this paper, we used polyvinylpyrrolidone (PVP) as a stabilizer to synthesize ultra-small Fe_3O_4 nanoparticles at 75°C by the coprecipitation method. For PVP molecules have pyrrolidone functional groups that can easily arrest crystals of Fe_3O_4 nanoparticles, they can help to form ultra-small magnetic particles and stop the aggregation of the nanoparticles. Lee et al. [19] prepared PVP-coated iron-oxide nanoparticles by the thermal decomposition of $Fe(CO)_5$ and confirmed their biocompatibility in MRI studies. Therefore, in this work, PVP was selected as a stabilizer instead of other commonly used dextran, starch, albumin and poly(ethyleneglycol) (PEG) in the current

Y. Zhang (✉) · S. Ma · Y.-J. Zhang · X.-D. Zhang · Z.-D. Zhang
Shenyang National Laboratory for Materials Science, Institute of Metal Research, and International Centre for Materials Physics, Chinese Academy of Sciences, 72 Wenhua Road, 110016 Shenyang, People's sRepublic of China
e-mail: yzhang7704@imr.ac.cn

Y. Zhang · J.-Y. Liu · X. Zhao
College of Pharmaceutical Engineering, Shen Yang Pharmaceutical University, 103 Wenhua Road, Shenyang 110016, People's Republic of China

X.-D. Zhang
College of Chemical Science and Engineering, Liao Ning University, Shenyang 110036, Peoples' Republic of China

coprecipitation method. The successful synthesis of the ultra-small Fe_3O_4 nanoparticles was confirmed by means of X-ray diffraction (XRD), transmission electron microscopy (TEM), infra spectrum (IR), and X-ray photoelectron spectroscopy (XPS). When exposed directly to biological environments, the ultra-small Fe_3O_4 magnetic nanoparticles presented biocompatibility and showed encouraging applications in MRI and magnetic delivery of drug.

2 Experimental

2.1 Materials

Polyvinylpyrrolidone (PVP, average MW: 7000–11000), ferrous sulfate (≥99.7%), iron sulfate (≥99.0%), and sodium hydroxide (≥96%) were purchased from SCRC. Water used in the experiment was distilled. All chemicals were used directly without further purification. The weight of laboratory mice was 18–22 g.

2.2 Synthesis of ultra-small Fe_3O_4 nanoparticles

The ultra-small Fe_3O_4 nanoparticles were synthesized by coprecipitation method [20]. 5.8 g of PVP was dissolved in 20 ml of distilled water. Then 5 ml of sodium hydroxide solution (3 M) was added into the PVP solution. Subsequently, the mixture of 2.5 ml of ammonium ferrous sulfate (0.5 M) and 5 ml of iron sulfate solution (0.5 M) was dripped into the PVP solution with dripping rate of 1.4 ml/min and PVP/Fe^{2+} molar ratio of 20/1 under the magnetic stirring and nitrogen protection. During the dripping process, the solution was gradually changed to black. The resulting black solution was maintained at 75°C for 1 h and then the solution was cooled to room temperature. Finally, the stable colloidal solution was obtained and the ultra-small Fe_3O_4 nanoparticles (PVP/Fe^{2+}: 20/1, sample-b) were separated by centrifugation at 9000 rpm for 10 min. In order to study the effect of dripping rates, other two samples with PVP/Fe^{2+} molar ratio of 20/1 (samples-c and -d) were also prepared according to this procedure, with the dripping rate of the solution 0.7 and 0.35 ml/min. In order to study the role of PVP molecules, the Fe_3O_4 nanoparticles (samples-e, -f and -a) with PVP/Fe^{2+} molar ratio of 10/1, 5/1 and 0/1 were prepared with the dripping rate of 0.35 ml/min. Detailed description of the experimental conditions is presented in Table 1.

2.3 In vivo MRI test

For in vivo MRI test of the PVP–Fe_3O_4 nanoparticles, the animals were anesthetized with an intramuscular injection of ketamine 35 mg/kg body weight. 0.2 ml of magnetic solution with PVP/Fe^{2+} molar ratio of 20/1 (30 mg/ml, sample-b) was injected into the tail vein of laboratory mice. Due to the high solubility and monodispersity of the magnetic particles in aqueous solution, we performed injection of magnetic solution without filtration. A columned 20 × 10 mm NdFeB permanent magnet with a field of 0.3 T was positioned next to the right side of liver for 30 min. Controlled animals were injected with ketamine without the presence of the permanent magnet. In vivo MRI was measured 1 h later.

2.4 Characterization and instrumentation

The powder XRD was performed at room temperature with a D/max 2400 X-ray diffractometer equipped with a Cu K_α radiation source ($\lambda = 0.154056$ nm). The morphology and size distribution of Fe_3O_4 nanoparticles were observed by using a JEOL 2010 TEM operating at 200 kV. XPS experiments were performed by using a commercial system (Thermo VG ESCALAB250 with MgK_α and Al K_α radiations) with a base pressure of 1×10^{-7} mbar. The T_2^*-weighted MR images of the mice were obtained with a turbo spin echo (TSE) technique using a 3 T MR machine (GE Excite). The sequence parameters were TR 920 ms, TE 83 ms, 1 mm thickness, and 8 × 8 cm field of view (FOV) (256 × 192 matrix, NEX = 4).

3 Results and discussion

The XRD patterns of the Fe_3O_4 nanoparticles prepared with PVP molecules are shown in Fig. 1. The XRD peaks

Table 1 Characterization results for prepared samples

PVP/Fe^{2+} Mole ratio	No.	Dripping rate (ml/min)	XRD and crystalline domain diameter (nm)		TEM	IR (CO)
20/1	b	1.4	Fig. 1b	6.5	Fig. 2b	
	c	0.7	Fig. 1c	3.1		
	d	0.35	Fig. 1d	1.9	Fig. 2a	1661
10/1	e	0.35		4.0		1632
5/1	f	0.35		5.6		1640
0/1	a	0.35	Fig. 1a	5.3		1661

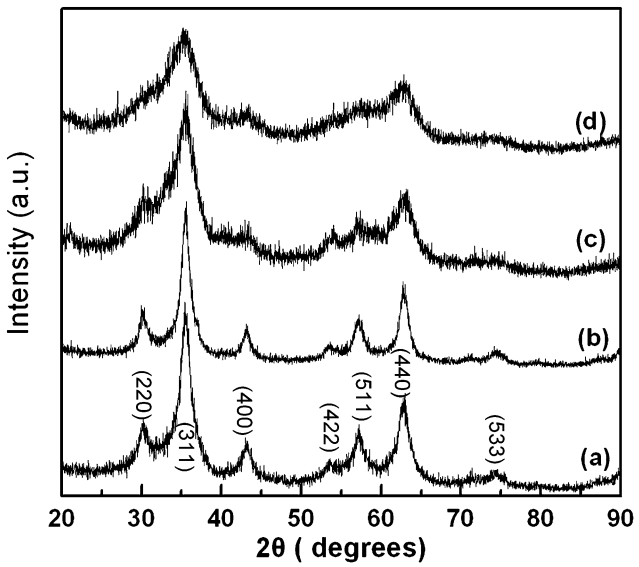

Fig. 1 XRD pattern of the samples: **a** non-PVP–Fe_3O_4; **b** PVP–Fe_3O_4-20/1, 1.4 ml/min; **c** PVP–Fe_3O_4-20/1, 0.7 ml/min; **d** PVP–Fe_3O_4-20/1, 0.35 ml/min

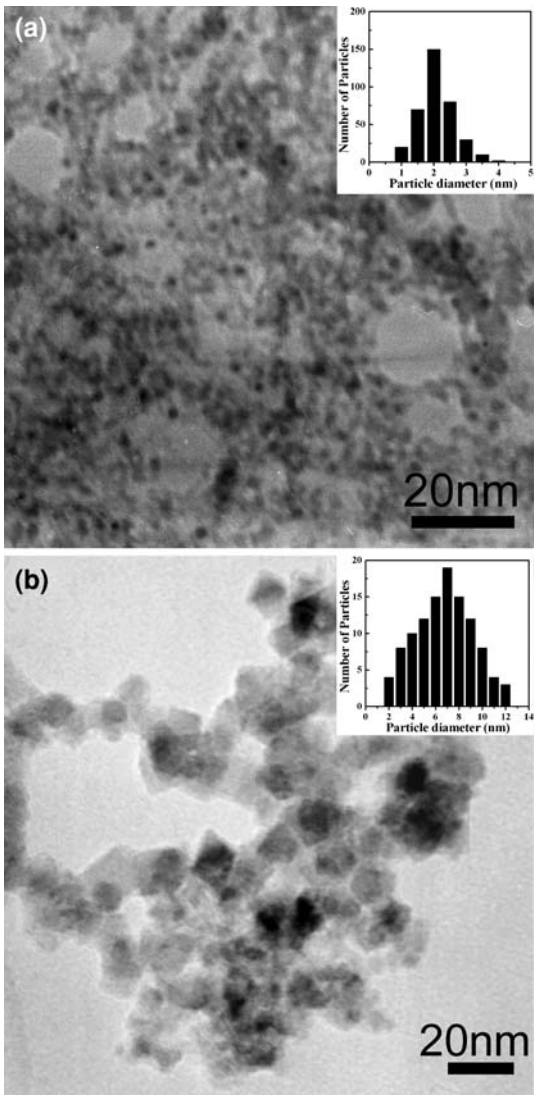

Fig. 2 TEM images of the samples: **a** PVP–Fe_3O_4-20/1, 0.35 ml/min;) PVP–Fe_3O_4-20/1, 1.4 ml/min

were consistent with those in the standard XRD pattern of Fe_3O_4 (No. 85-1436), which confirmed the crystallinity of Fe_3O_4 nanoparticles. Furthermore, by using the Scherrer's equation, the crystalline grain diameters of the Fe_3O_4 particles were calculated according to the (311) XRD peak. With increasing the dripping rate from 0.35 to 1.4 ml/min, the crystalline grain diameters of the Fe_3O_4 particles (samples-d, -c and -b) increased from 1.9 to 6.5 nm. The crystalline grain diameter of the Fe_3O_4 particles (sample-a) prepared with dripping rate of 0.35 ml/min and PVP/Fe^{2+} molar ratio of 0/1, was calculated as 5.3 nm. It was noticed that the diameter (5.3 nm) of sample-a was almost three times that of sample-d (1.9 nm), which indicated that PVP molecules may help to decrease the size of the Fe_3O_4 particles. With increasing PVP/Fe^{2+} molar ratio from 5/1 to 20/1, the crystalline grain size of iron-oxide core decreased from 5.6 to 1.9 nm. Lee et al. [19] reported that the size of PVP coated iron-oxide nanocomposites increased from 119 to 417 nm (measured by ELS) with the increase of PVP/[$Fe(CO)_5$] molar ratio from 0.125 to 0.5. As a kind of macromolecule stabilizer, PVP molecules may act as space block or space bridge to stabilize particles [21]. The amount of PVP determined the mode. When the PVP amount increased and PVP/Fe^{2+} molar ratio reached 5/1, PVP molecules may be more likely to act as space block. As a result, in this work, the smallest Fe_3O_4 particles could be prepared with lowest dripping rate of 0.35 ml/min and PVP/Fe^{2+} molar ratio of 20/1.

Figure 2a, b showed TEM images of the Fe_3O_4 particles (samples-d and -b) synthesized with dripping rate of 0.35 and 1.4 ml/min and PVP/Fe^{2+} molar ratio of 20/1, respectively. The morphologies of samples-d and -b showed spherical shape and rhombohedral shape, respectively, with homogeneous dispersed distribution. The average sizes of the Fe_3O_4 particles were determined from Fig. 2a, b to be 2 and 7 nm, respectively, which are close to the crystalline grain values calculated by using Scherrer's equation (samples-d and -b). The slight difference may be due to the presence of multi-grain particles.

The FT-IR spectra of PVP coated Fe_3O_4 nanoparticles and pure PVP were shown in Fig. 3. With increasing PVP/Fe^{2+} molar ratio from 0/1 to 10/1, the CO bands shifted from 1661 to 1632 cm^{-1}. The results indicated the chemical interaction between CO groups and the Fe_3O_4 nanoparticles. In addition, the interaction increased with the decrease of the particle size, which can be attributed to the surface effect of nanoparticles. When PVP/Fe^{2+} molar

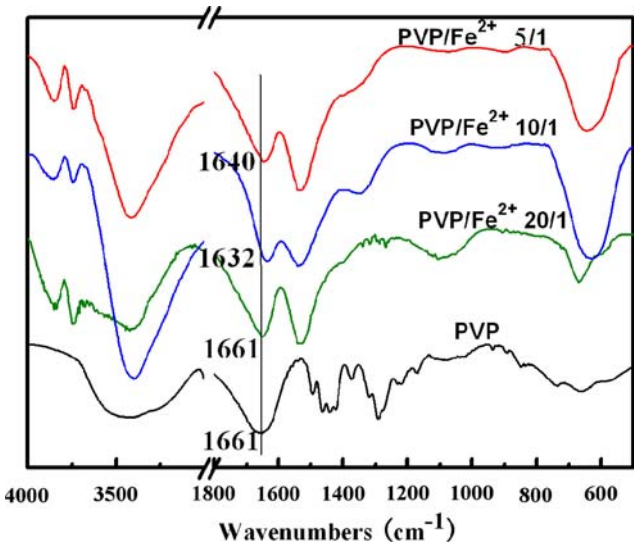

Fig. 3 Infrared spectra of the samples: **a** neat PVP; **b** PVP–Fe_3O_4-5/1; **c** PVP–Fe_3O_4-10/1; **d** PVP–Fe_3O_4-20/1

ratio reached 20/1, the CO bands peaked at 1661 cm^{-1} and no shift was observed. It indicated that large excessive PVP remained on this sample, probably just remained free on the surface, despite the successive washing steps were done after the synthesis. It is the excessive free PVP molecules that prevent the aggregation of the magnetic particles as indicated by TEM. Therefore, for preparing the well dispersed PVP coated Fe_3O_4 particles, the effective concentration of PVP is 20 times that of Fe^{2+}.

Figure 4a, b showed XPS spectra of sample-d with etching time 0 and 30 s, respectively. The C1s, N1s, O1s and Fe2p peaks indexed at 285, 400, 532 and 722 eV, respectively, indicated the existence of PVP and Fe_3O_4. With increasing the etching time, the intensity of C and N decreased (Table 2), which revealed that the excessive free PVP molecules lost. When the etching time reached 30 s, the intensity of Fe reached maximum, which suggested that the surface of Fe_3O_4 had been reached. In order to study the interaction of PVP molecules and Fe_3O_4 nanoparticles, the XPS spectrum with etching 30 s was selected for discussion. The XPS spectrum of C1s was decomposed into four peaks by the multiple Gaussians curve fitting, as shown in Fig. 4c. The peaks at 285.0, 285.2, 286.2 and 289.2 eV indicated carbon atoms with number 1–4 in different chemical environments (see the inset of Fig. 4c). Comparing the XPS spectrum of carbon atoms of number 4 with that of pure PVP (288.6 eV), the present peak at 289.2 eV shifted to higher binding energy. This result indicated the interaction between the carboxyl (C=O) groups and the Fe_3O_4 nanoparticles. The peak at 531.4 eV can be attributed to carboxyl (C=O) oxygen in PVP repeated unit. The peak at 400.0 eV can be due to nitrogen atoms. No obvious shifts of O1s and N1s peaks were observed, which suggested that the oxygen and nitrogen atoms in PVP had no

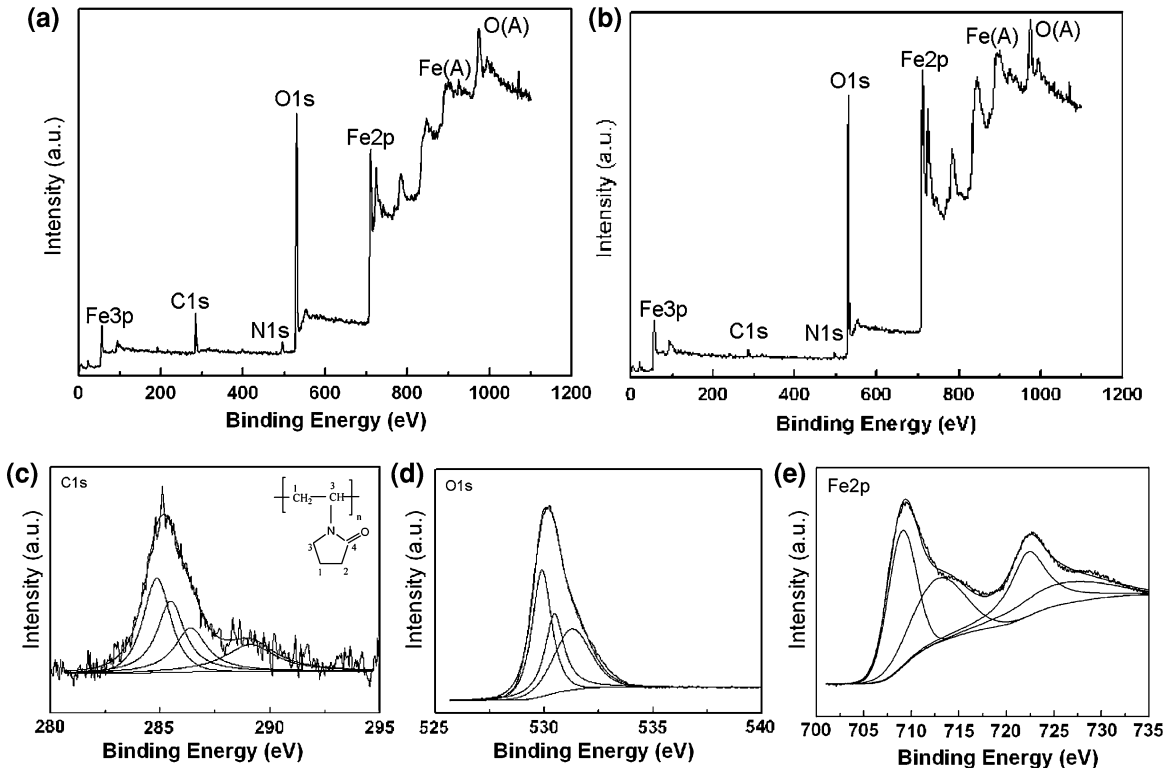

Fig. 4 XPS spectra of PVP–Fe_3O_4-20/1 **a** in whole range with deeping time 0 s; **b** in whole range with deeping time 30 s **c** C1s; **d** O1s; **e** Fe2p

Table 2 Etch time and atomic percent (%)

Etch time (s)	Peaks atomic percent (%)			
	C1s	N1s	O1s	Fe2p
0	26.6437	1.29744	57.8487	14.2101
15.015	10.3587	0.389196	65.417	23.8351
30.015	8.097	0.315665	65.2655	26.3218

markedly chemical interaction with the Fe_3O_4 particle core. Therefore, the carbon atoms in carboxyl group contribute to the interaction between the PVP molecules and the Fe_3O_4 nanoparticles.

The XPS spectrum of Fe atoms was shown in Fig. 4e. The peaks at 723.2 and 709.9 eV were in accordance with Fe 2p1/2 and 2p3/2 of different oxidation states in Fe_3O_4. The Fe 2p1/2 peak in the PVP coated Fe_3O_4 nanoparticles was lower than that of Fe atoms in pure Fe_3O_4 (723.8 eV), which indicated the interaction between Fe atoms and the polymeric ligands. In addition, the lower binding energy peak of Fe 2p1/2 suggested that electron clouds around carbon atoms of carboxyl (CO) groups intended to be close to Fe atoms in Fe_3O_4 nanoparticles. The peaks at 529.9 and 530.5 eV can be indexed to oxygen atoms in the PVP coated Fe_3O_4 nanoparticles. In comparison with O1s peaks (529.1 and 529.6 eV) of pure Fe_3O_4, the O1s peaks of the PVP coated Fe_3O_4 nanoparticles appeared to shift toward higher binding energy, which may be caused by the interaction between the Fe atoms and carboxyl (C=O) groups of PVP. Therefore, the interaction between the PVP molecules and the Fe_3O_4 nanoparticles was the excursion of the electron clouds from C atoms (in CO) to Fe atoms.

This kind of interaction, from the view of valence bond theory, can be interpreted as coordination bond. For the requirement of special configuration of iron coordination compounds, the growth of the Fe_3O_4 nanoparticles was restrained. Therefore, as a stabilizer, PVP molecules covering on the surface of Fe_3O_4 nanoparticles play the role of restraining the growth of Fe_3O_4 nanoparticles. Jiang et al. [22] reported that the presence of PVP was essential to prevent the aggregation and growth of the nanoparticles in PVP-mediated polyol reduction process. In our study, the function of PVP is in accordance with the previous result.

To observe the in vivo MRI effect, T_2-weighted MRI was performed in laboratory mice. Compared with Fig. 5a, the PVP coated Fe_3O_4 nanoparticles obviously exhibited negative contrast enhancement for lung, liver and kidney as shown in Fig. 5b. In addition, in Fig. 5b, PVP coated Fe_3O_4 nanoparticles concentrated in target, which is due to the attraction of the magnet. Therefore, the in vivo results showed that PVP coated Fe_3O_4 nanoparticles could be concentrated at the target area guided by the permanent magnet and obviously exhibited negative contrast enhancement for the whole body.

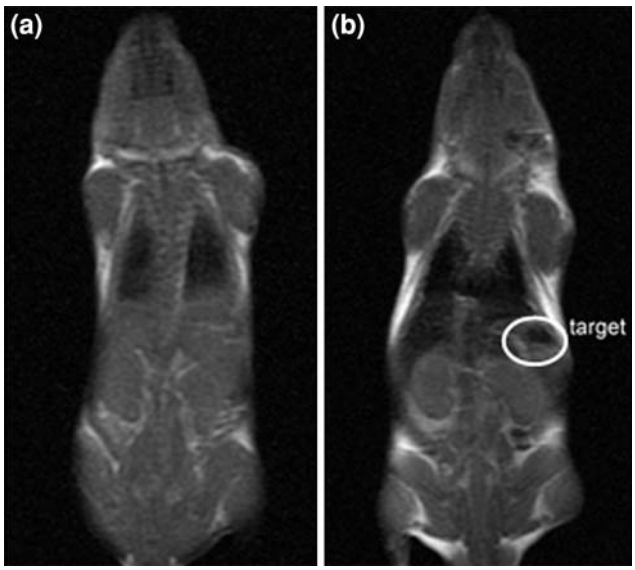

Fig. 5 Magnetic resonance imaging of mice following intra-arterial injection of PVP–Fe_3O_4. **a** The image of mice without injecting ferrofluids and magnetic field; **b** the image of mice injected PVP–Fe_3O_4 with magnetic field target at right side of liver

4 Conclusions

Ultra-small Fe_3O_4 magnetic nanoparticles were synthesized by coprecipitation method with PVP as a stabilizer. In synthetic conditions, PVP molecules not only prevent the aggregation of the Fe_3O_4 nanoparticles, but also restrict their size by utilizing the interaction between the carbon atoms in carbonyl groups and the Fe atoms on the Fe_3O_4 nanoparticles. The as-prepared Fe_3O_4 nanoparticles with diameter from 6.5 to 1.9 nm were homogeneous and well dispersed. In vivo results for MRI and magnetic targeting showed that the PVP coated Fe_3O_4 particles could be concentrated at the target area and obviously exhibited negative contrast enhancement for the whole body. Therefore, the PVP coated Fe_3O_4 particles prepared by the present method would have encouraging applications in MRI and magnetic delivery of drug [1, 23] and should be investigated further.

Acknowledgments This work was supported by National Natural Science Foundation of China under Grant No. 50331030 and 50831006.

References

1. Zhang ZD. Nanocapsules. In: Nalwa HS, editor. Encyclopedia of nanoscience and nanotechnology, vol. 6. Stevenson Ranch, CA: American Scientific Publishers; 2004. p. 77–160.

2. Gu HW, Xu KM, Xu CJ, Xu B, Biofunctional magnetic nanoparticles for protein separation and pathogen detection. Chem Commun. 2006;941–9. doi:10.1039/b514130c.
3. Oscar BM, María PM, Pedro T, Jesus RC, Pierre B, Martín S, et al. Fe-based nanoparticles metallic alloys as contrast agents for 395 magnetic resonance imaging. Biomaterials. 2005;26:5695–703. doi:10.1016/j.biomaterials.2005.02.020.
4. Xie HY, Zuo C, Liu Y, Zhang ZL, Pang DW, Li XL, et al. Cell-targeting multifunctional nanospheres with both fluorescence and magnetism. Small. 2005;1:506–9. doi:10.1002/smll.200400136.
5. Tanaka H, Sugita T, Yasunaga YJ, Shimose SJ, Deie M, Kubo T, et al. Efficiency of magnetic liposomal transforming growth factor-β 1 in the repair of articular cartilage defects in a rabbit model. J Biomed Mater Res. 2005;73A:255–63. doi:10.1002/jbm.a.30187.
6. Yang Y, Jiang JS, Du B, Gan ZF, Qian M, Zhang P. Preparation and properties of a novel drug delivery system with both magnetic and biomolecular targeting. J Mater Sci Mater Med. 2009;20:301–7. doi:10.1007/s10856-008-3577-0.
7. Gou ML, Qian ZY, Wang H, Tang YB, Huang MJ, Kan B, et al. Preparation and characterization of magnetic poly(ε-caprolactone)-poly(ethyleneglycol)-poly(ε-caprol -actone) micro-spheres. J Mater Sci Mater Med. 2008;19:1033–41. doi:10.1007/s10856-007-3230-3.
8. Lu Y, Yin Y, Mayers BT, Xia YN. Modifying the surface properties of superparamagnetic iron oxide nanoparticles through a sol–gel approach. Nano Lett. 2002;2:183–6. doi:10.1021/nl015681q.
9. Si S, Kotal A, Mandal TK, Giri S, Kohara T. Size-controlled synthesis of magnetite nanoparticles in the presence of polyelectrolytes. Chem Mater. 2004;16:3489–96. doi:10.1021/cm049205n.
10. Wan SR, Huang JS, Yan HS, Liu KL. Size-controlled preparation of magnetite nanoparticles in the presence of graft copolymers. J Mater Chem. 2006;16:298–303. doi:10.1039/b512605c.
11. Sun S, Zeng H. Size-controlled synthesis of magnetite nanoparticles. J Am Chem Soc. 2002;124:8204–5. doi:10.1021/ja026501x.
12. Liz L, Lopez Quintela MA, Mira J, Rivas J. Preparation of colloidal Fe_3O_4 ultrafine particles in microemulsions. J Mater Sci. 1994;29:3797–801. doi:10.1007/BF00357351.
13. Lee HS, Lee WO. A comparison of coprecipitation with microemulsion methods in the preparation of magnetite. J Appl Phys. 1999;85:5231–3. doi:10.1063/1.369953.
14. Liu ZL, Wang X, Yao KL, Du GH, Lu QH, Ding ZH, et al. Synthesis of magnetite nanoparticles in W/O microemulsion. J Mater Sci. 2004;39:2633–6. doi:10.1023/B:JMSC.0000020046.68106.22.
15. Lee YJ, Lee JW, Bae CJ, Park JG, Noh HJ, Park JH, et al. Large-scale synthesis of uniform and crystalline magnetite nanoparticles using reverse micelles as nanoreactors under reflux conditions. Adv Func Mater. 2005;15:503–9. doi:10.1002/adfm.200400187.
16. Chin AB, Yaacob II. Synthesis and characterization of magnetic iron oxide nanoparticles via w/o microemulsion and Massart's procedure. J Mater Process Tech. 2007;191:235–7. doi:10.1016/j.jmatprotec.2007.03.011.
17. Sasmita M, Nabakumar P, Samrat M, Sudip KG, Panchanan P. A simple synthesis of amine-derivatised superparamagnetic iron oxide nanoparticles for bioapplications. J Mater Sci. 2007;42:7566–74. doi:10.1007/s10853-007-1597-7.
18. Zhang Y, Wang SN, Ma S, Guan JJ, Li D, Zhang XD, et al. Self-assembly multifunctional nanocomposites with Fe_3O_4 magnetic core and CdSe/ZnS quantum dots shell. J Biomed Mater Res. 2008;85A:840–6. doi:10.1002/jbm.a.31609.
19. Lee HY, Lim NH, Seo JA, Yuk SH, Kwak BK, Khang G, et al. Preparation and magnetic resonance imaging effect of polyvinylpyrrolidone-coated iron oxide nanoparticles. J Biomed Mater Res. 2006;79B:142–50. doi:10.1002/jbm.b.30524.
20. Zhang Y, Liu JJ, Yang F, Zhang YJ, Yao Q, Cui TY, et al. A new strategy for assembling multifunctional nanocomposites with iron oxide and amino-terminated PAMAM dendrimers. J Mater Sci Mater Med. 2009. doi: 10.1007/s10856-009-3808-z.
21. Ren J, Shen J, Lu SC. Dispersion and regulation of particles in liquid phase. In: Xing T, editor. Dispersion science and technology of particles. Beijing: Chemical Industry Press; 2005. p. 199.
22. Jiang P, Zhou JJ, Li R, Gao Y, Sun TL, Zhao XW, et al. PVP-capped twinned gold plates from nanometer to micrometer. J Nanopart Res. 2006;8:927–34. doi:10.1007/s11051-005-9046-5.
23. Zhang ZD. Magnetic nanocapsules. J Mater Sci Tech. 2007;23:1–14.